

# Three-domain architecture of stress-free epitaxial ferroelectric films

A. L. Roytburd<sup>a)</sup> and S. P. Alpay<sup>b)</sup>

*Department of Materials and Nuclear Engineering, University of Maryland, College Park, Maryland 20742*

L. A. Bendersky

*Materials Science and Engineering Laboratory, National Institute of Standards and Technology, Gaithersburg, Maryland 20899*

V. Nagarajan and R. Ramesh

*Department of Materials and Nuclear Engineering, University of Maryland, College Park, Maryland 20742*

(Received 27 June 2000; accepted for publication 2 October 2000)

Epitaxial ferroelectric films undergoing a cubic-tetragonal phase transformation relax internal stresses due to the structural phase transformation and the difference in the thermal expansion coefficients of the film and the substrate by forming polydomain structures. The most commonly observed polydomain structure is the *c/a/c/a* polytwin which only partially relieves the internal stresses. Relatively thicker films may completely reduce internal stresses if all three variants of the ferroelectric phase are brought together such that the film has the same in-plane size as the substrate. In this article, we provide experimental evidence on the formation of the three-domain structure based on transmission electron microscopy in 450 nm thick (001)  $\text{PbZr}_{0.2}\text{Ti}_{0.8}\text{O}_3$  films on (001)  $\text{SrTiO}_3$  grown by pulsed laser deposition. X-ray diffraction studies show that the film is fully relaxed. Experimental data is analyzed in terms of a domain stability map. It is shown that the observed structure in epitaxial ferroelectric films is due to the interplay between relaxation by misfit dislocations at the deposition temperature and relaxation by polydomain formation below the phase transformation temperature. © 2001 American Institute of Physics. [DOI: 10.1063/1.1328781]

## I. INTRODUCTION

Polydomain (polytwin) formation in epitaxial films undergoing a phase transformation is a mechanism that relaxes internal stresses that are a result of the lattice misfit due to the structural phase transformation and the difference in the thermal expansion coefficients of the film and the substrate. This phenomenon has been predicted theoretically<sup>1</sup> and was studied to epitaxial ferroelectric films and multilayer heterostructures.<sup>2–6</sup> The polydomain structure of tetragonal epitaxial ferroelectric films consists of the three possible orientational domains of the tetragonal phase separated from each other by elastically compatible 90° domain walls. Figure 1(a) shows all possible orientational variants of the ferroelectric phase and possible polydomain structures due to a cubic-tetragonal transformation. Ferroelectric films are deposited at temperatures above the transition temperature and the internal stresses are usually completely relaxed by misfit dislocations at this temperature.<sup>3,7</sup> There are no significant thermal stresses during cooling down since the difference between the thermal expansion coefficients of  $\text{PbTiO}_3$  and tetragonal  $\text{PbZr}_x\text{Ti}_{1-x}\text{O}_3$  (PZT) solid solutions and popular perovskite substrates such as  $\text{SrTiO}_3$  and  $\text{LaAlO}_3$  is very small. Thus, just before the structural phase transformation at  $T_C$ ,

the films are stress-free and tensile internal stresses develop just below  $T_C$  due to the phase transformation. Therefore, the most common microstructure observed in epitaxial films  $\text{PbTiO}_3$  (Ref. 2) and tetragonal PZT solid solutions<sup>8</sup> is the *c/a/c/a* polydomain consisting of alternating thin platelets of *c* domains with the tetragonal axis perpendicular to the film–substrate interface and *a* domains with the *c* axis of the tetragonal film along [100] or [010] directions, called  $a_1$  and  $a_2$  domains, respectively [Fig. 1(b)].

The *c/a/c/a* polytwin structure only partially relaxes the internal stresses by reducing the biaxial stress state to a uniaxial one. The internal stresses due to lattice misfit can be *completely* reduced if all of the three variants of the tetragonal phase are arranged such that the film has the same in-plane size as the substrate.<sup>1,9–11</sup> In this article, we present experimental results that confirm the existence of three-domain structures in epitaxial ferroelectric films and we show that the internal stresses in these ferroelectric films are indeed completely relaxed. The experimental data is analyzed using a domain stability map.

## II. THEORY

If a ferroelectric film is grown epitaxially on a thick cubic substrate such that  $(001)_{\text{film}} // (001)_{\text{substrate}}$ , the misfit due to the difference in lattice parameters of the film and the substrate may be described by the following misfit strain tensors for  $a_1$ ,  $a_2$ , and *c* domains, respectively, as

<sup>a)</sup>Corresponding author; electronic mail: royburd@wam.umd.edu

<sup>b)</sup>Currently with Department of Metallurgy and Materials Engineering, University of Connecticut, Storrs, CT 06269; electronic mail: p.alpay@ims.uconn.edu

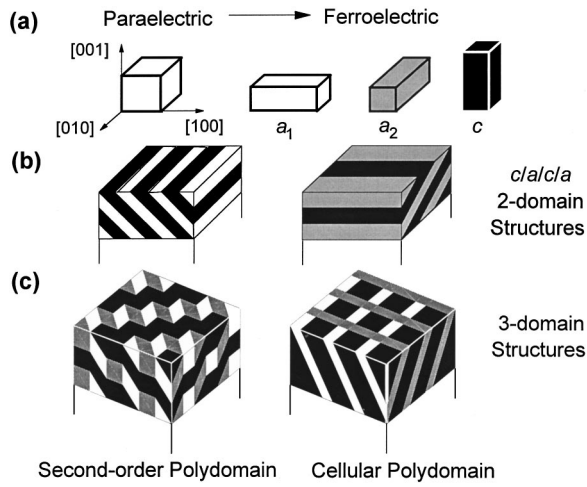


FIG. 1. (a) Cubic paraelectric phase and the three ferroelectric tetragonal variants, (b) the simple two-domain  $c/a/c/a$  polydomain structures, and (c) the three-domain architectures; second-order polytwin and the cellular arrangement of the domains.

$$\hat{\epsilon}_1^M = \begin{pmatrix} \epsilon_T' & 0 & 0 \\ 0 & \bar{\epsilon}_M & 0 \\ 0 & 0 & \bar{\epsilon}_M \end{pmatrix}, \quad \hat{\epsilon}_2^M = \begin{pmatrix} \bar{\epsilon}_M & 0 & 0 \\ 0 & \epsilon_T' & 0 \\ 0 & 0 & \bar{\epsilon}_M \end{pmatrix}, \quad \hat{\epsilon}_3^M = \begin{pmatrix} \bar{\epsilon}_M & 0 & 0 \\ 0 & \bar{\epsilon}_M & 0 \\ 0 & 0 & \epsilon_T' \end{pmatrix}, \quad (1)$$

where  $\epsilon_T' = \bar{\epsilon}_M + \epsilon_T$ ,  $\bar{\epsilon}_M = (a - \bar{a}_S)/\bar{a}_S$  is the effective misfit strain,  $\epsilon_T = (c/a)/a$  is the tetragonality of the ferroelectric lattice,  $a$  and  $c$  are the unconstrained lattice parameters of the film, and  $\bar{a}_S$  is the effective substrate lattice parameter<sup>3,6</sup> given in terms of the equilibrium linear dislocation density  $\rho$  at the deposition temperature  $T_G$  as

$$\bar{a}_S(T) = \frac{a_S(T)}{\rho(T_G)a_S(T) + 1}. \quad (2)$$

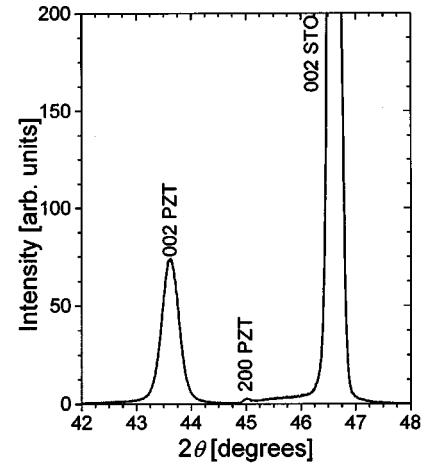
For a homogeneous mixture of domains, the condition for complete relaxation of the average stress is  $\langle \epsilon_{xx} \rangle = \langle \epsilon_{yy} \rangle = 0$ , where  $\langle \epsilon_{xx} \rangle$  and  $\langle \epsilon_{yy} \rangle$  are the average strains along [100] and [010] directions, i.e.,

$$\alpha_1 \hat{\epsilon}_1^M + \alpha_2 \hat{\epsilon}_2^M + \alpha_3 \hat{\epsilon}_3^M = \begin{pmatrix} 0 & 0 & 0 \\ 0 & 0 & 0 \\ 0 & 0 & (\alpha_1 + \alpha_2)\bar{\epsilon}_M + \alpha_3\epsilon_T' \end{pmatrix}. \quad (3)$$

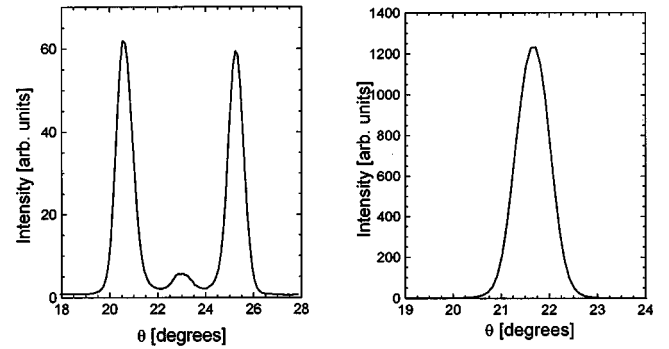
Here,  $\alpha_1$ ,  $\alpha_2$ , and  $\alpha_3$  are the volume fractions of  $a_1$ ,  $a_2$ , and  $c$  domains, respectively ( $\alpha_1 + \alpha_2 + \alpha_3 = 1$ ). Full relaxation is attained for  $\alpha_1 = \alpha_2$ , and

$$\alpha_3 = \frac{2\bar{\epsilon}_M}{\epsilon_T} + 1, \quad (4)$$

if  $-(\epsilon_T/2) < \bar{\epsilon}_M < 0$ . The resultant domain structure is due to (i) relaxation by misfit dislocations at  $T_G$  and (ii) relaxation by polydomain formation below the transformation tempera-



(a)



(b)

(c)

FIG. 2. (a) XRD pattern of the sample in the 40°–50° range, (b) 200  $\theta$  rocking curve, and (c) 002  $\theta$  rocking curve.

ture  $T_C$ . These two different mechanisms are taken into account through the dislocation density dependence of the misfit strain, i.e.,  $\bar{\epsilon}_M$ , and the tetragonality,  $\epsilon_T$ .

The architecture of the three-domain structures is dictated by the energy of the interdomain interfaces, the energy of the junctions where the three domains come together, and by the microstresses at the film–substrate interface. Microstresses are created because of the periodic deviation of the actual misfit from the average misfit on the film–substrate interface.<sup>12</sup> These factors increase the total energy of the system although the elastic energy of macrostresses<sup>13</sup> is effectively reduced to zero. Their interplay results in a critical thickness below which the three-domain state is not stable.<sup>9</sup> It can be shown that the second-order polydomain structure is favored for small  $c$ -domain fractions,  $\alpha_3$ , whereas for relatively larger  $\alpha_3$ , the cellular arrangement is more stable [see Fig. 1(c)]. A complete theoretical treatment of the three-domain structures will be presented in a future article.

### III. EXPERIMENTAL RESULTS AND DISCUSSION

Experimentally, 450 nm thick (001)  $\text{PbZr}_{0.2}\text{Ti}_{0.8}\text{O}_3$  (PZT 20/80) films on (001)  $\text{SrTiO}_3$  (STO) substrates were deposited at 650 °C and 100 mTorr oxygen partial pressure by

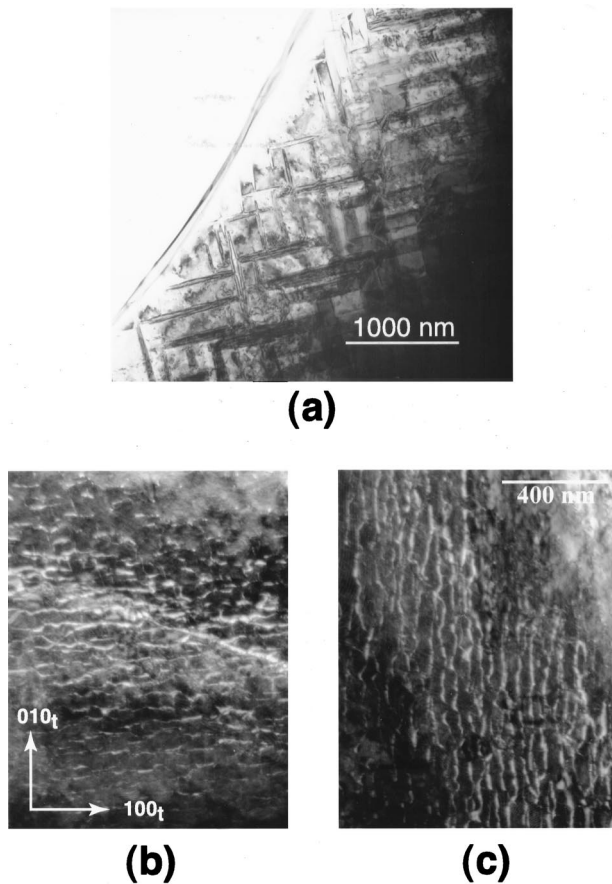


FIG. 3. (a) Bright field micrograph taken from a plan-view TEM sample showing the cellular arrangement of all the three domains; two dark field images taken with (b) (100) and (c) (010) reflections. Spacing between the dislocations is  $\sim 40$  nm.  $\mathbf{g} \times \mathbf{b}$  criteria and visibility of the dislocation lines suggests Burgers vectors of the dislocations to be  $\mathbf{b}=[010]$  and  $\mathbf{b}=[100]$ .

pulsed laser deposition. The details of the deposition procedure were given elsewhere.<sup>14</sup> X-ray diffraction (XRD) experiments for all samples were done on a four-circle Siemens D5000 diffractometer with monochromatic Cu  $K_\alpha$  radiation with a Ni filter to remove Cu  $K_\beta$  diffractions. Crystallographic characterization was accomplished with standard  $\theta$ - $2\theta$  scans,  $\theta$  rocking curves, and  $\phi$  scans. Epitaxial growth in the samples was established from  $\phi$  scans and the presence of only 00l type reflections in the  $\theta$ - $2\theta$  diffraction pattern. A Phillips 430 transmission electron microscope (TEM) operated at 300 keV was employed to obtain plan-view microstructures. The samples were prepared by dimpling and ion milling from the substrate side and were not cooled during ion milling.

The  $\theta$ - $2\theta$  diffraction pattern in the  $40^\circ$ - $50^\circ$  range is shown in Fig. 2(a). The lattice parameters calculated from the 200 and 002  $\theta$ - $2\theta$  diffraction of PZT 20/80 give  $a = 0.3930$  nm and  $c = 0.4130$  nm, very close to their respective bulk values,<sup>15</sup> indicating that the epitaxial stresses are completely relieved. The fraction of  $c$  domains is approximately 0.80, established from the relative integrated intensities of the 200 and 002 PZT  $\theta$  rocking curves [Figs. 2(b) and 2(c), respectively] following the methodology of Hsu and Raj<sup>16</sup> and Kang *et al.*<sup>17</sup>

The plan-view TEM micrograph in Fig. 3(a) displays the

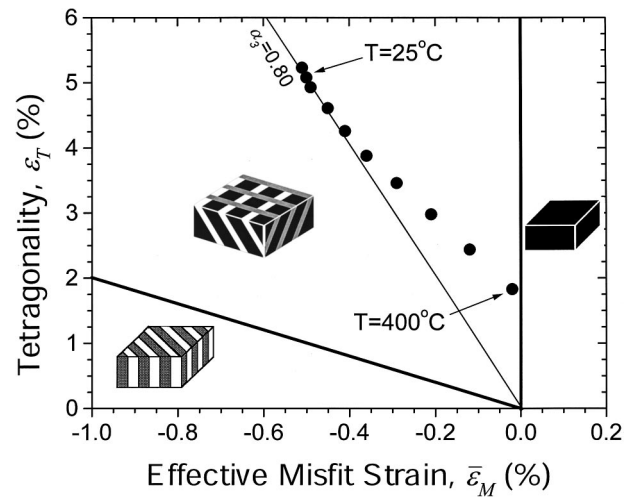


FIG. 4. Domain stability map for 450 nm thick (001) PZT 20/80 films on (001) STO substrates. Filled circles represent the expected position of the theoretical effective misfit strain and tetragonality pairs at different temperatures from 25 to 400 °C. On the thin line in the three-domain region (equifraction line), the  $c$ -domain fraction is constant and is equal to 0.80.

microstructure that consists of all the three possible domains of the tetragonal ferroelectric phase. The film is divided into cells of  $c$  domains in the (001) plane bound by  $a_1$  and  $a_2$  domains along the [100] and [010] directions, respectively. It should be noted that since the interdomain interfaces may be inclined by  $45^\circ$  or  $135^\circ$  with respect to the [100] or [010] directions, these cells are not rectangular boxes. Their exact three-dimensional geometry depends on the specific crystallographic planes of the interdomain interfaces. The  $c$  domain fraction is consistent with XRD results and the fraction of  $a_1$  and  $a_2$  domains are equal as predicted theoretically. Furthermore, the micrographs in Figs. 3(b)-3(c) reveal the presence a pseudo-orthogonal network of misfit dislocations with Burgers vectors  $\mathbf{b}=[100]$  and  $\mathbf{b}=[010]$ . Spacing between dislocations is  $\sim 40$  nm, corresponding to a linear density of  $0.0025 \text{ nm}^{-1}$ .

Since the tetragonality for PZT 20/80 is approximately 5.2%<sup>15</sup> and the observed  $c$ -domain fraction is  $\sim 0.80$ ,  $\bar{\epsilon}_M = (a - \bar{a}_S) / \bar{a}_S$  should be equal to  $\sim 0.5\%$ . Therefore,  $\bar{a}_S$  should be 0.3954 nm at room temperature (compared to the bulk lattice parameter of STO which is 0.3905 nm<sup>15</sup>), corresponding to a 73% relaxation by misfit dislocations when extrapolated to the deposition temperature (thermal expansion coefficient of STO =  $11 \times 10^{-6} \text{ }^\circ\text{C}^{-1}$ ). The theoretical linear dislocation density is approximately  $0.0030 \text{ nm}^{-1}$ , in good agreement with experimental observation. The results can be elegantly combined on a domain stability map as shown in Fig. 4 using the effective misfit strain concept and the temperature dependencies of the lattice parameters of the film and the substrate. The domain stability is constructed by comparing the total elastic energies of all possible single domain and polydomain structures following the formalism of our previous article.<sup>6</sup> Full theoretical derivation leading to the domain stability map and its analysis will be given elsewhere. It can be shown that  $a_1$ - and  $a_2$ -single domains are not stable for any given pair of  $\bar{\epsilon}_M$  and  $\epsilon_T$ . Furthermore, the  $c/a/c/a$  polytwins are also unstable because for any pair of

$\bar{\epsilon}_M$  and  $\epsilon_T$ , their energy is always larger than either the single domain  $c$ , the  $a_1/a_2/a_1/a_2$  polydomain, or the three-domain structure. The lower and upper limits of the  $c$ -domain fraction  $\alpha_3$  [see Eq. (3)] for the three-domain structure define the phase stability boundaries between  $a_1/a_2/a_1/a_2$  and the three-domain state and the three-domain state and the single domain  $c$ , respectively ( $\alpha_3=0$ , i.e.,  $\epsilon_1=-2\epsilon_M$ , and  $\alpha_3=1$ , i.e.,  $\epsilon_M=0$ ). Within the stability area of the three-domain structure,  $\alpha_3$  gradually changes from 0 to 1 as the misfit approaches 0.

To compare theoretical analysis with experimental results, the effective misfit strain and tetragonality pairs for the PZT 20/80 film on a STO substrate are evaluated at different temperatures and their respective positions on the domain stability map are marked (see Fig. 4, full circles). On the thin line given by  $\epsilon_T=-10\times\bar{\epsilon}_M$ ,  $\alpha_3$  is constant and is equal to 0.80 [see Eq. (3)]. This line passes through the point [ $\bar{\epsilon}_M(25^\circ\text{C}), \epsilon_T(25^\circ\text{C})$ ], indicating that the  $c$ -domain fraction is  $\sim 0.80$  at room temperature.  $\alpha_3$  increases with increasing temperature since the slopes of the equifraction lines approach the vertical axis given by  $\bar{\epsilon}_M=0$ .

The domain structure shown in Fig. 3(a) may play an important role in the switching characteristics of ferroelectric films. Recently, we have demonstrated experimentally that the switching in (001) PZT 20/80 films on (001) LaAlO<sub>3</sub> substrates proceeds faster in thicker films ( $\sim 400$  nm) compared to thinner films of thickness  $h\leq 100$  nm under pulsed testing conditions.<sup>14</sup> The so-called activation field  $E_\alpha$ , a measure of the impedance to switching,<sup>18,19</sup> fell substantially as the film thickness was increased. The microstructure of the films observed via TEM changed from a single-domain state ( $h<60$  nm) to a polydomain structure ( $h\geq 60$  nm) with gradual decline in the  $c$ -domain fraction coupled with increase in the density of  $90^\circ$  domain walls. The polydomain formation was accompanied by a drop in the saturation polarization and relaxation of internal stresses.<sup>20</sup> Although it is difficult to single out the formation of polydomain structure as the only reason for faster switching in these films with increasing  $h$ , together with atomic force microscope studies that show heterogeneous nucleation of reversed domains at  $90^\circ$  domain walls in 400 nm PZT 20/80 films on STO substrates,<sup>21</sup> it is reasonable to hypothesize that they have a distinct contribution to the process of polarization reversal. However, it may be due to a pure size effect or it may be related to the different internal stress levels in the films.

#### IV. CONCLUSION

We have shown that in epitaxial tetragonal ferroelectric films, the internal stresses may be completely relaxed with

the formation of a polydomain structure that consists of all the three variants of the ferroelectric tetragonal phase. TEM observations prove the existence of such structures and XRD studies show that the internal stresses are indeed relieved by the creation of the three-domain architectures. A domain stability map is constructed that takes into account the possibility of the formation of the three-domain structures. Theoretically predicted domain fraction is in excellent agreement with experimental results. In a future article, we will present a full thermodynamic treatment of the formation of three-domain structure and analyze its effect on the electrical and electromechanical properties.

#### ACKNOWLEDGMENTS

The authors gratefully acknowledge the support by the National Science Foundation (NSF) under Grant No. DMR-9903279 and by the NSF-MRSEC program under Grant No. DMR-9632521.

- <sup>1</sup>A. L. Roytburd, *Phys. Status Solidi A* **37**, 329 (1976).
- <sup>2</sup>B. S. Kwak, A. Erbil, J. D. Budai, M. F. Chrisholm, L. A. Boatner, and B. J. Wilkens, *Phys. Rev. B* **49**, 14865 (1994).
- <sup>3</sup>J. S. Speck and W. Pompe, *J. Appl. Phys.* **76**, 466 (1994).
- <sup>4</sup>N. A. Pertsev and A. G. Zembilgotov, *J. Appl. Phys.* **78**, 6170 (1995).
- <sup>5</sup>N. Sridhar, J. M. Rickman, and D. J. Srolovitz, *Acta Mater.* **44**, 4085; 4097 (1996).
- <sup>6</sup>S. P. Alpay and A. L. Roytburd, *J. Appl. Phys.* **83**, 4714 (1998).
- <sup>7</sup>S. P. Alpay, V. Nagarajan, L. A. Bendersky, M. D. Vaudin, S. Aggarwal, R. Ramesh, and A. L. Roytburd, *J. Appl. Phys.* **85**, 3271 (1999).
- <sup>8</sup>C. M. Foster, G. R. Bai, R. Csencsits, J. Vetrone, R. Jammy, L. A. Wills, E. Carr, and J. Amano, *J. Appl. Phys.* **81**, 2349 (1997).
- <sup>9</sup>A. L. Roytburd and Y. Yu, *Ferroelectrics* **144**, 137 (1993).
- <sup>10</sup>S. P. Alpay and A. L. Roytburd, in *Epitaxial Oxide Thin Films III*, edited by C. M. Foster, J. S. Speck, D. G. Schlom, C. B. Eom, and M. E. Hawley [Mater. Res. Soc. Symp. Proc. **474**, 407 (1997)].
- <sup>11</sup>A. L. Roytburd, in *Thin Film Ferroelectric Materials and Devices*, edited by R. Ramesh (Kluwer Academic, Norvell, MA, 1997), p. 71.
- <sup>12</sup>A. L. Roytburd, *J. Appl. Phys.* **83**, 239 (1998).
- <sup>13</sup>A. L. Roytburd, *J. Appl. Phys.* **83**, 228 (1998).
- <sup>14</sup>V. Nagarajan, I. G. Jenkins, S. P. Alpay, H. Li, S. Aggarwal, L. Salamanca-Riba, A. L. Roytburd, and R. Ramesh, *J. Appl. Phys.* **86**, 595 (1999).
- <sup>15</sup>Landolt-Börnstein, in *Numerical Data and Functional Relationships in Science and Technology*, edited by K.-H. Hellwege and A. M. Hellwege (Springer, Berlin, 1981), Vol. 16.
- <sup>16</sup>W.-Y. Hsu and R. Raj, *Appl. Phys. Lett.* **67**, 792 (1995).
- <sup>17</sup>Y. M. Kang, J. K. Ku, and S. Baik, *J. Appl. Phys.* **78**, 2601 (1995).
- <sup>18</sup>W. J. Merz, *J. Appl. Phys.* **27**, 938 (1956).
- <sup>19</sup>E. Fattuzo and W. J. Merz, *J. Appl. Phys.* **32**, 1685 (1961).
- <sup>20</sup>A. L. Roytburd, S. P. Alpay, V. Nagarajan, C. S. Ganpule, S. Aggarwal, E. D. Williams, and R. Ramesh, *Phys. Rev. Lett.* **85**, 190 (2000).
- <sup>21</sup>C. S. Ganpule, V. Nagarajan, H. Li, A. S. Ogale, D. E. Steinhauer, S. Aggarwal, E. Williams, R. Ramesh, and P. De Wolf, *Appl. Phys. Lett.* **77**, 292 (2000).